Emirati Journal of Civil Engineering and Applications
Vol 2 Issue 2 (2024)
Pages (12 - 18)

Available at www.emiratesscholar.com

Investigating the Compressive Response of Hand-Laminated GFRP Pipes in the Hoop Direction through Experiment and FEM Modeling

Yasir Zaman[1], Fayiz Amin[2], Muhammad Asif[:] , Khan Abdul Majid [3] Niazi Ehsanullah[4]
iamyasirzaman@gmail.com, fayizamin092@gmail.com, asifkmuhammad123@gmail.com, abdulmajidk693@gmail.com, ahsanniazi@qq.com
Faculty of Mechanical Engineering, Ghulam Ishaq Khan Institute, Topi 23460, Pakistan.[1]
Faculty of Civil Engineering, Ghulam Ishaq Khan Institute, Topi 23460, Pakistan.[2]
Xi'an University of Technology, Shaanxi, Xi'an, Beilin, Jinhua S Rd, 710048, China.[3]
China three gorges University Yichang hubei.[4]

ARTICLE INFO

Published on 8th of August 2024
Doi: 10.54878/z6xyr883

KEYWORDS

GFRP Pipe, Compression Test, Hand Lay Method, Composites, FEM Modeling, Abaqus

HOW TO CITE

Investigating the Compressive Response of Hand-Laminated GFRP Pipes in the Hoop Direction through Experiment and FEM Modeling. (2024). Emirati Journal of Civil Engineering and Applications, 2(2), 11-18

ABSTRACT

Composite materials represent a relatively recent development with compelling attributes such as lightweight and high durability, making them increasingly appealing for diverse engineering applications, notably in aerospace. This study investigates the compressive performance of a hand-layup manufactured composite glass fiber reinforced polymer pipe. Experimental compression tests were conducted following ASTM guidelines using a universal testing machine (UTM). Mechanical responses under axial compression were evaluated for hoop orientation, with analysis of fracture surfaces revealing various damage mechanisms including debonding, whitening, matrix cracking, delamination, and fiber splitting. The study reports a maximum compressive strength of 6.88 MPa and a Young's modulus of 382.24 MPa in the hoop direction, with the maximum load sustained being 6.797 kN. Furthermore, the model was validated using the Finite Element Analysis in Abaqus, which showed good alignment between the experimental findings and the FEM modeling results. This work provides insights that are potentially useful for applications in the aerospace sector.

1. Introduction

Composite materials have become increasingly popular in engineering use because of their impressive specific strength, stiffness, and ability to withstand fatigue [1]. Glass fiber-reinforced polymer pipes are now seen as advantageous substitutes for traditional steel piping, mainly due to their improved strength-to-weight ratio, cost efficiency, and ease of large-scale production [2]. Glass fiber pipes are utilized in a range of industries, such as aerospace [3], chemical processing [4], water and wastewater management [5], [6], the oil and gas sector [7], desalination plants [8], power generation [9], and the mining and milling processing industry [10].

The study by Mohamed S. Abd-Elwahed et al. [11] aimed to optimize the machining parameters, including spindle speed, feed rate, and laminate thickness, for drilling woven-glass-fiber reinforced epoxy composites using response surface analysis. The research identified optimal parameters, such as a 0.025 mm/rev feed rate and 1600 rpm spindle speed for a 5.4 mm laminate thickness, which were consistent with the experimental findings. Angelo Gaetani's et al. [12] research developed a numerical procedure to efficiently fill the computational domain with diverse point sets, improving the accuracy of the analysis, particularly in tensile loading scenarios. This approach was validated through parametric simulations that compared the predicted mechanical properties and failure modes against experimental findings. Valentino Paolo Berardi et al. [13] investigated the long-term viscous behavior of unidirectional glass fiber reinforced polymer laminates manufactured using the wet lay-up technique. The study examined the creep characteristics of these composite materials and their individual constituents. S. J. Smith et al. [14] developed finite-element models to simulate the behavior of GFRP pultruded member joints. Their models closely matched the experimentally measured elastic stiffnesses, demonstrating the reliability of their approach in modeling joint behavior under diverse loading conditions.

Kasidit Chansawat et al. [15] conducted a study utilizing three-dimensional finite element models to simulate the behavior of reinforced concrete beams strengthened with glass and carbon fiber-reinforced polymer sheets. The study validated these computational models against experimental data, confirming qualitative consistency in the structural behavior and crack initiation patterns observed under loading until failure. Julio F. Davalos et al. [16] research focused on developing long-term durability prediction models for glass fiber-reinforced polymer (GFRP) bars used in concrete environments. Their study emphasized the accelerated degradation of these materials due to factors such as moisture exposure and elevated temperatures, particularly at the critical fiber/matrix interface. The researchers highlighted the crucial factors that influence the long-term performance of GFRP materials in such applications. Salwa E.L. Garouge et al. [17] investigated the influence of fiber orientation and stacking sequence on the mechanical properties of glass/epoxy composite panels. The research focused on applications in the naval industry, where composites offer substantial mechanical advantages, particularly under dynamic water impact conditions.

Prior research has extensively explored the relaxation properties of various composite materials. However, there remains a gap in knowledge regarding the compressive behavior of hand-laminated GFRP pipes specifically under hoop loading. This study addresses this novelty by investigating the compressive strength of GFRP (Glass Fiber Reinforced Polymer) pipes, a material widely utilized in the aerospace industry, particularly for drone arms. These pipes encounter demanding operational environments characterized by payload weight, thrust and motor forces, vibrations and oscillations, wind and weather effects, impact and collision risks, variations in altitude and air density, and exposure to extreme temperatures.

2. Methodology:

The research methodology involves a multi-step approach. The first step is the fabrication of GFRP pipes using the Hand Lay Method. This is followed by the execution of compressive tests in hoop directions, conducted on a universal testing machine and adhering to ASTM D695-91 standards. The subsequent phase involves the numerical modeling of the GFRP pipe using the FEM software ABAQUS. The final step encompasses the validation and comparison of the experimental findings with the results obtained from the FEM modeling.

2.1. Fabrication of GFRP Pipe

The GFRP pipe was fabricated using 50 grams of Weave Ultra-Light Woven Glass. The production process employed a hand lay-up method, where 40%

of the total weight of the glass fiber was used for the epoxy. The epoxy resin and hardener were mixed in a 2:1 ratio. The epoxy mixture was then manually distributed evenly through the glass fibers. Subsequently, the reinforced fibers were wrapped around a PVC pipe with an outer diameter of 31.5 mm (about 1.24 in) and a length of 80 mm (about 3.15 in) and sealed with tape. The assembly was left to set for 7-8 hours. After this period, the PVC pipe was removed, yielding the GFRP pipe. Figure 1 shows the fabrication of GFRP Pipe.

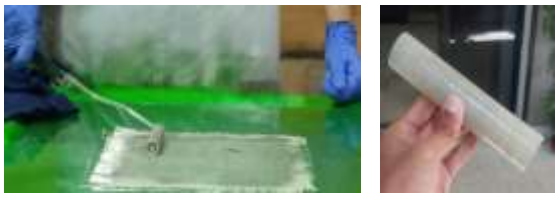

Figure 1: (a) Manufacturing of GFRP Pipe by Hand Lay Method (b) Glass Fiber Reinforced Polymer GFRP Pipe

2.2. Experimental Test

The compressive strength test is performed using a 20 kN universal testing machine. The specimen, with dimensions specified in Table 1, is positioned such that its bottom surface rests on the fixed, lower platen of the machine, which is constrained in all directions to prevent any displacement or rotation. The upper platen of the machine, which is restricted to moving only vertically, is in contact with the top surface of the specimen and applies the compressive load. The compressive force is continuously increased until the specimen fails, and all test data is recorded by the computer for analysis.

Geometry	**Dimensions (mm)**
Length	80
Outer Diameter	35.5
Inner Diameter	31.5
Thickness	2

Table 1 Geometric Details of the GFRP Pipe

Figure 2 depicts the specimen undergoing a compression test in a Universal Testing Machine (UTM).

Figure 2 (a) GFRP Pipe under universal testing machine UTM (b) GFRP Pipe after Compression Test

2.3. Modeling of GFRP Pipe

The research further suggests conducting a detailed numerical modeling study of the GFRP pipe, replicating the same geometry, boundary conditions, loading, and material properties as in the experimental investigation. This numerical modeling should employ the Hashin damage criteria [18] to identify an appropriate modeling approach for the GFRP pipe. The Hashin 2D criterion is integrated into the ABAQUS software. The four failure modes considered are presented below.

Fiber Tension ($\sigma_{11} \geq 0$)

$$F_f^t = \left(\frac{\sigma_{11}}{X^t}\right)^2 + \alpha \left(\frac{\sigma_{12}}{S^L}\right)^2 \qquad 2.1$$

Fiber Compression ($\sigma_{11} \leq 0$)

$$F_f^c = \left(\frac{\sigma_{11}}{X^c}\right)^2 \qquad 2.2$$

Matrix Tension ($\sigma_{22} \geq 0$)

$$F_m^t = \left(\frac{\sigma_{22}}{Y^t}\right)^2 + \left(\frac{\sigma_{12}}{S^L}\right)^2 \qquad 2.3$$

Matrix Compression ($\sigma_{22} \leq 0$)

$$F_m^c = \left(\frac{\sigma_{22}}{2S^T}\right)^2 + \left[\left(\frac{Y^c}{2S^T}\right)^2 - 1\right]\left(\frac{\sigma_{22}}{Y^c}\right) + \left(\frac{\sigma_{12}}{S^L}\right)^2 \qquad 2.4$$

In equations (2.1) -(2.4), σ_{ij} (i,j = 1,2) represent the components of the effective stress tensor. X^t (X^c) and Y^t (Y^c) denote the tensile (compressive) strengths of uni-directional laminates in the longitudinal and transverse directions, respectively. Additionally, S^j (j =

L, T) corresponds to the in-plane and out-of-plane shear strengths of the composites. For any of the failure modes, $F_i^j = 1\ (i = f,\ m\ and\ j = c, t)$ indicates the onset of failure in that mode.

2.3.1. Geometric Details

A finite element (FE) representation of the GFRP pipe was developed within the Abaqus software, utilizing the dimensional specifications detailed in Table 2.

Geometry	Dimensions (mm)
Length	80
Shell Diameter	35.5

Table 2 Geometric Details

Figure 3 offers a visual representation of the model's intricate geometric configuration.

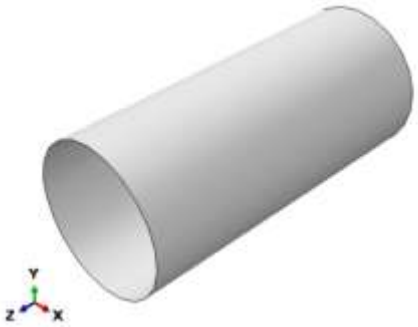

Figure 3 Geometry of the GFRP Pipe in Abaqus

2.3.2. Materials

Glass Fiber Reinforced Polymer (GFRP) demonstrates anisotropic mechanical behavior [19]. This signifies a directional dependence of its material properties, resulting in variations in response to applied stress or force depending on the direction of application. The mechanical properties are illustrated in Table 3 [20].

2.3.3. Loading and Boundary Conditions

The compressive load is applied evenly across one edge of the specimen's shell in the finite element analysis (FEA) software, with the loading rate steadily increasing. One end of the specimen is designated for loading of 20KN and moves downward to apply the compressive force. This end is permitted to move only vertically to ensure axial compression. In contrast, the opposite end is fixed and does not move, being constrained in all directions, preventing any displacement or rotation. Figure 4(a) shows loading and boundary conditions.

2.3.4. Meshing

Meshing is a crucial step in finite element modeling, as it involves discretizing the complex solid geometry into smaller, more manageable elements or cells. The size and quality of the mesh significantly impacts the accuracy of the simulation results. To ensure the mesh is appropriate for the analysis, a mesh convergence study was conducted, and the findings are presented in the subsequent sections. The meshed geometry of the model is depicted in Figure 4(b).

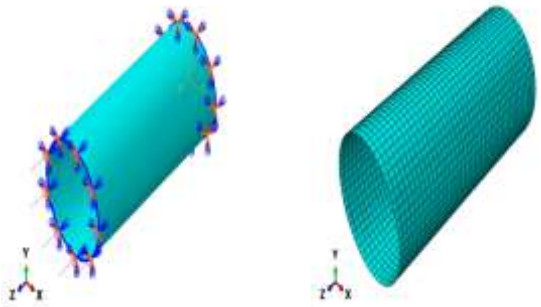

Figure 4 (a) Loading and Boundary Conditions of GFRP Pipe (b) Meshing Geometry of GFRP Pipe

3. Results and Discussion

3.1. Testing Results of GFRP Pipe

Figure 6 shows the experimental results for stress-strain and load-deflection of the GFRP pipe subjected to hoop loading.

The analysis of the plotted data reveals impressive strength in the hoop direction. The pipe boasts a maximum compressive strength of 6.88 MPa, indicating a remarkable ability to withstand compression. Furthermore, the high Young's Modulus of 382.24 MPa in the hoop direction signifies exceptional stiffness against deformation in this plane. This translates to the pipe's strong resistance to bending and maintaining its shape under pressure.

Engineering Constant		**Constitutive Damage Model Parameters of Lamina**	
E_{11}, GPa	36.9	Longitudinal Tensile Strength, MPa	820
E_{22}, GPa	10	Longitudinal Compressive Strength, MPa	500
E_{33}, GPa	10	Transverse Tensile Strength, MPa	80.6
G_{12}, GPa	3.3	Transverse Compressive Strength, MPa	322
G_{13}, GPa	3.3	Longitudinal Shear Strength, MPa	54.5
G_{23}, GPa	3.6	Transverse Shear Strength, MPa	161.2
V_{12}	0.32	Longitudinal Tensile Fracture Energy, N/mm	32
V_{13}	0.32	Longitudinal Compressive Fracture Energy, N/mm	20
V_{23}	0.44	Transverse Tensile Fracture Energy, N/mm	4.5
		Transverse Compressive Fracture Energy, N/mm	4.5

Table 3 Material Properties of the GFRP

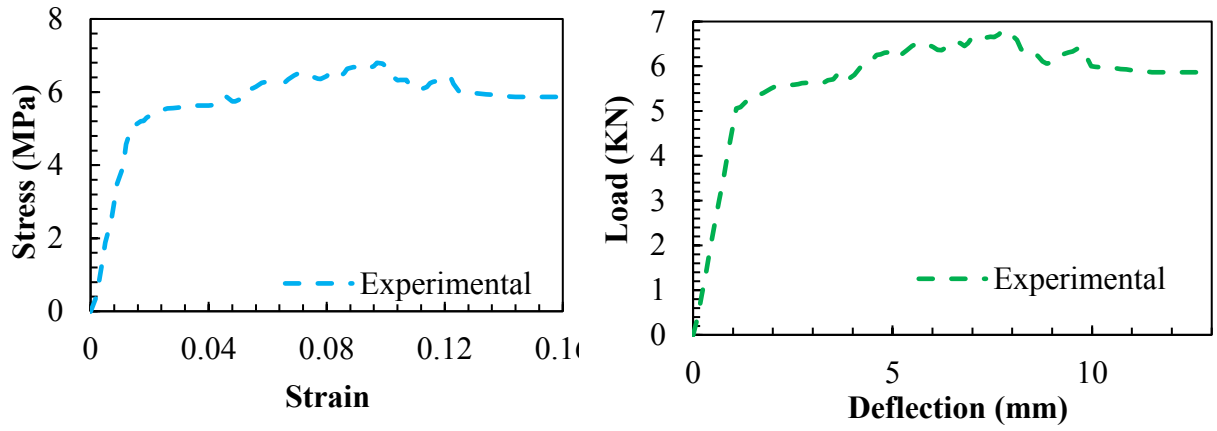

Figure 6 (a) Experimental Stress Vs Stain Curve (b) Experimental Load Vs Deflection Curve

3.2. Comparison of Experimental and FEM Modeling

Figure 7 presents a comparative analysis of the compression test results for the GFRP pipe, derived from both experimental procedures and FEM modeling. Specifically, Figure 7(a) illustrates the comparison of the stress-strain curve for the GFRP pipe while Figure 7(b) depicts the load versus deflection curve, highlighting the correspondence between the experimental and FEM modeling data.

The comparison reveals a close agreement between the experimental response and the numerical model's predictions. This finding confirms the efficacy of FEM in accurately determining the compressive strength of the GFRP pipe.

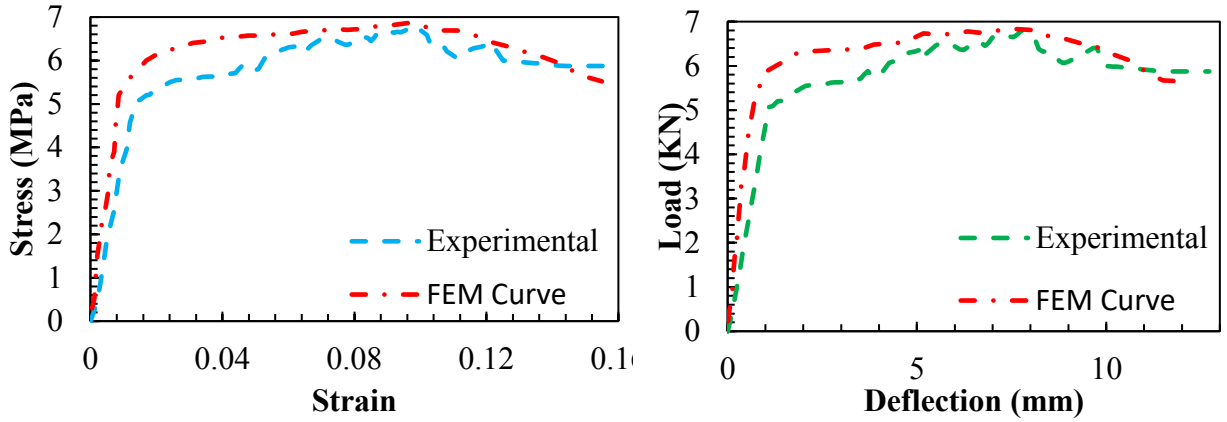

Figure 7 (a) Comparison of Stress Vs Stain Curve (b) Comparison of Load Vs Deflection Curve

4. Conclusion

This study combined experimental and computational approaches to assess the compressive behavior of hand-laminated glass fiber reinforced polymer (GFRP) pipes subjected to hoop loading. The experimental phase utilized a universal testing machine to acquire empirical data on the compressive strength of the GFRP pipes. Finite element modeling, implemented through Abaqus software, served as the computational component. A comparative analysis was subsequently conducted to evaluate the consistency between the experimentally obtained results and the modeling outputs. The analysis confirmed the suitability of the GFRP pipes' compressive strength for applications within the aerospace industry, such as drone arms. The findings revealed that the GFRP pipes exhibited a significant enhancement in compressive strength, reaching a value of 6.88 MPa in the hoop direction and a maximum sustainable load of 6.797 kN were observed. These results contribute to the existing knowledge base and hold promise for the incorporation of GFRP pipes within the aerospace sector.

Some recommendations for future research are outlined below:

- Compression test in the radial direction: Future research should incorporate compression tests in the radial direction to assess the material's performance under radial loadings.
- Explore manufacturing techniques: The impact of different manufacturing techniques on the mechanical properties of GFRP pipes should be explored.
- Study material combinations: The performance of GFRP pipes in combination with other materials should be studied to enhance their properties for specific applications.

References

1. "Glass-Fiber Reinforced Plastic - an overview | ScienceDirect Topics." Accessed: Jun. 15, 2024. [Online]. Available: https://www.sciencedirect.com/topics/materials-science/glass-fiber-reinforced-plastic
2. T. Raghav Arvind, D. Roshann Ram Dayal, K. L. H. Krishna, and S. Survesh, "Mechanical characterization and comparison of glass fibre and glass fibre reinforced with aluminium alloy (GFRAA) for automotive application," Mater Today Proc, vol. 46, pp. 1181–1186, Jan. 2021, doi: 10.1016/J.MATPR.2021.02.062.
3. B. Parveez, M. I. Kittur, I. A. Badruddin, S. Kamangar, M. Hussien, and M. A. Umarfarooq, "Scientific Advancements in Composite Materials for Aircraft Applications: A Review," Polymers 2022, Vol. 14, Page 5007, vol. 14, no. 22, p. 5007, Nov. 2022, doi: 10.3390/POLYM14225007.
4. L. E. McCandlish, B. H. Kear, and B. K. Kim, "Chemical processing of nanophase WC–Co composite powders," https://doi.org/10.1179/026708390790189641, vol. 6, no. 10, pp. 953–957, Oct. 1990, doi: 10.1179/026708390790189641.

5. I. Luhar et al., "A State-of-the-Art Review on Innovative Geopolymer Composites Designed for Water and Wastewater Treatment," Materials 2021, Vol. 14, Page 7456, vol. 14, no. 23, p. 7456, Dec. 2021, doi: 10.3390/MA14237456.
6. M. A. Dutt, M. A. Hanif, F. Nadeem, and H. N. Bhatti, "A review of advances in engineered composite materials popular for wastewater treatment," J Environ Chem Eng, vol. 8, no. 5, p. 104073, Oct. 2020, doi: 10.1016/J.JECE.2020.104073.
7. M. Roseman, R. Martin, and G. Morgan, "Composites in offshore oil and gas applications," Marine Applications of Advanced Fibre-Reinforced Composites, pp. 233–257, Jan. 2016, doi: 10.1016/B978-1-78242-250-1.00010-7.
8. A. S. Alsaman, E. M. M. Ibrahim, M. S. Ahmed, and A. A. Askalany, "Composite adsorbent materials for desalination and cooling applications: A state of the art," Int J Energy Res, vol. 46, no. 8, pp. 10345–10371, Jun. 2022, doi: 10.1002/ER.7894.
9. Y. Chen, "Glass Fiber-Reinforced Polymer Composites for Power Equipment," Polymer Composites for Electrical Engineering, pp. 377–417, Jan. 2021, doi: 10.1002/9781119719687.CH13.
10. A. I. Azmi, R. J. T. Lin, and D. Bhattacharyya, "Tool wear prediction models during end milling of glass fibre-reinforced polymer composites," International Journal of Advanced Manufacturing Technology, vol. 67, no. 1–4, pp. 701–718, Jul. 2013, doi: 10.1007/S00170-012-4516-2/METRICS.
11. M. S. Abd-Elwahed, "Drilling Process of GFRP Composites: Modeling and Optimization Using Hybrid ANN," Sustainability 2022, Vol. 14, Page 6599, vol. 14, no. 11, p. 6599, May 2022, doi: 10.3390/SU14116599.
12. A. Gaetani, A. Fascetti, and N. Nisticò, "Parametric investigation on the tensile response of GFRP elements through a discrete lattice modeling approach," Compos B Eng, vol. 176, p. 107254, Nov. 2019, doi: 10.1016/J.COMPOSITESB.2019.107254.
13. V. P. Berardi, M. Perrella, L. Feo, and G. Cricrì, "Creep behavior of GFRP laminates and their phases: Experimental investigation and analytical modeling," Compos B Eng, vol. 122, pp. 136–144, Aug. 2017, doi: 10.1016/J.COMPOSITESB.2017.04.015.
14. S. J. Smith, I. D. Parsons, and K. D. Hjelmstad, "Finite-Element and Simplified Models of GFRP Connections," Journal of Structural Engineering, vol. 125, no. 7, pp. 749–756, Jul. 1999, doi: 10.1061/(ASCE)0733-9445(1999)125:7(749).
15. T. H. Miller, K. Chansawat, T. Potisuk, S. C. Yim, and D. I. Kachlakev, "FE Models of GFRP and CFRP Strengthening of Reinforced Concrete Beams," Advances in Civil Engineering, vol. 2009, no. 1, p. 152196, Jan. 2009, doi: 10.1155/2009/152196.
16. J. F. Davalos, Y. Chen, and I. Ray, "Long-term durability prediction models for GFRP bars in concrete environment," http://dx.doi.org/10.1177/0021998311427777, vol. 46, no. 16, pp. 1899–1914, Nov. 2011, doi: 10.1177/0021998311427777.
17. S. E. L. Garouge, M. Tarfaoui, O. Hashim Hassoon, H. E. L. Minor, and A. Bendarma, "Effect of stacking sequence on the mechanical performance of the composite structure under slamming impact," Mater Today Proc, vol. 52, pp. 29–39, Jan. 2022, doi: 10.1016/J.MATPR.2021.10.109.
18. Z. Hashin, "Failure Criteria for Unidirectional Fiber Composites," J Appl Mech, vol. 47, no. 2, pp. 329–334, Jun. 1980, doi: 10.1115/1.3153664.
19. V. G. Martynenko, G. I. Lvov, and Y. N. Ulianov, "Experimental investigation of anisotropic viscoelastic properties of glass fiber-reinforced polymeric composite material," Polymers and Polymer Composites, vol. 27, no. 6, pp. 323–336, Jul. 2019, doi: 10.1177/0967391119846362/ASSET/IMAGES/LARGE/10.1177_0967391119846362-FIG9.JPEG.
20. S. S. R. Koloor, A. Karimzadeh, N. Yidris, M. Petrů, M. R. Ayatollahi, and M. N. Tamin, "An Energy-Based Concept for Yielding of Multidirectional FRP Composite Structures Using a Mesoscale Lamina Damage Model," Polymers 2020, Vol. 12, Page 157, vol. 12, no. 1, p. 157, Jan. 2020, doi: 10.3390/POLYM12010157.